Inorganic Chemistry

Article

pubs.acs.org/IC

Topochemical Cross-Linking of the $[Hf_2N_2]$ Layers with Sulfur in α-HfNBr

Shuai Zhang, Mayumi Yoshikawa, Kei Inumaru, and Shoji Yamanaka*

Department of Applied Chemistry, Graduate School of Engineering, Hiroshima University, Higashi-Hiroshima 739-8527, Japan

ABSTRACT: α-HfNBr (space group *Pmmn*) isostructural with FeOCl consists of orthorhombic $[Hf_2N_2]$ layers sandwiched by bromide layers. By the reaction with Na_2S at 750 °C in a sealed glass tube, the α-type $[Hf_2N_2]$ layers are topochemically cross-linked with sulfur to form α-Hf_2N_2S with a mutual shift of the layers in the *ab* plane by $(a/2 + b/2)$ to crystallize in space group *Immm* and the lattice parameters $a = 4.1422(1)$, $b = 3.5058(1)$, and $c = 11.4043(3)$ Å. At a higher reaction temperature of 850 °C, the β-type layered variant β-Hf_2N_2S with a double honeycomb network is obtained, which adopts the La_2O_2S structure with space group $P\bar{3}m1$ and the lattice parameters $a = 3.5805(1)$ and $c = 6.4063(1)$ Å.

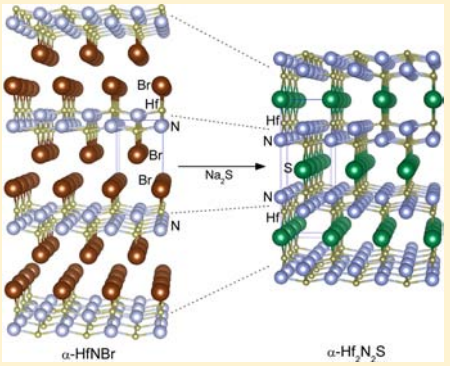

INTRODUCTION

Metal nitride halides MNX (M = Ti, Zr, Hf; X = Cl, Br, I) provide a versatile material system rich in superconducting materials as well as crystal chemistry. There are two types of layered polymorphs for MNX: the α- and the β-type isomorphous with FeOCl and SmSI, respectively.[1−3] Both structures are composed of double metal nitride layers $[M_2N_2]$ sandwiched by halogen layers, $X[M_2N_2]X$; the nitride layers of the different types have different structures within the layers, orthogonal and honeycomb networks for the α- and the β-type, respectively, as schematically shown in Figure 1. MNX compounds are band insulators with a gap of 3−4 eV.[4,5] Upon electron doping by intercalation of alkali,[6−9] alkaline earth and rare earth metals,[10,11] or organic bases,[12,13] most of the compounds are changed into superconductors with relatively high transition temperatures (T_c's). The highest T_c (25.5 K) has been observed for the lithium and THF (tetrahydrofuran) co-intercalated β-HfNCl, $Li_{0.48}(THF)_yHfNCl$, with a basal spacing of 17.8 Å.[6,8] TiNCl with the α-type layered structure can form intercalation compounds with various amines as well as alkali metals;[12,14] the octamethylenediamine intercalated compound shows a T_c of 17.1 K.[13] The superconductivity occurs within the thin molecular nitride layers of MNX, and the superconducting mechanisms are considered to be different for the different types of layered host structures.[8,15,16]

The superconducting metal-nitride layers $[M_2N_2]$ can be swelled with organic solvent molecules upon co-intercalation with metal atoms, and the basal spacing expands to a value larger than 30 Å.[8,11,13,17] On the other hand, the chlorine atoms in β-ZrNCl are topochemically deintercalated, keeping the layered network of β-$[Zr_2N_2]$, which is changed into a stacking of thin ZrN layers with the rock salt structure.[18] We focus on the robustness of the $[M_2N_2]$ layers as building units for use in nanoscale molecular engineering. Stoltz et al. have derived β-$[Zr_2N_2]S$ from β-ZrNCl by substitution of chloride layers with sulfide layers, where the β-type $[Zr_2N_2]$ honeycomb layers are alternately stacked with the closely packed sulfide layers; sulfur atoms occupy all of the octahedral sites coordinated by six

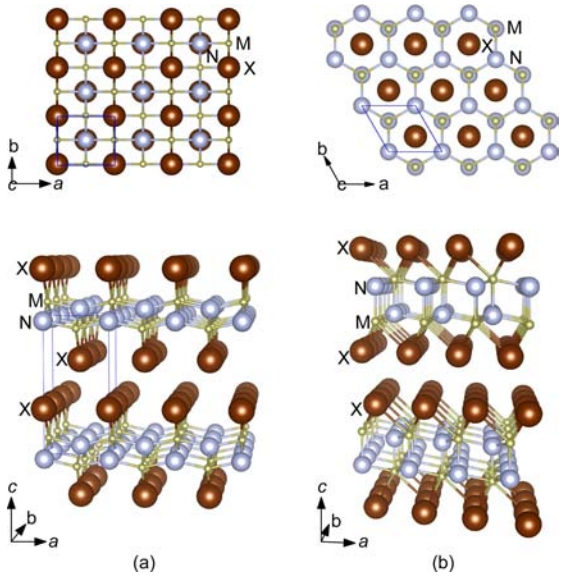

Figure 1. Schematic illustration of the two types of structures of the α-type (a) and the β-type (b) MNX (M = Ti, Zr, Hf; X = Cl, Br, I). The upper parts show the views along the *c* axis (in-plane arrangements of the nitride layers), and the lower parts along the *b* axis (stacking of the nitride layers).

Received: June 19, 2013
Published: August 27, 2013

   dx.doi.org/10.1021/ic401548a | *Inorg. Chem.* 2013, 52, 10571−10575

zirconium atoms, [Zr−N−N−Zr]S[Zr−N−N−Zr].[18] The interlayer partial structure [Zr−S−Zr] of β-Zr_2N_2S is isostructural with Hf_2S with space group $P6_3/mmc$.[19,20] In this study, the α-type $[Hf_2N_2]$ orthogonal layers of α-HfNBr have been successfully cross-linked with sulfur atoms. The sulfide layers are loosely packed and arranged so as to form a new tunnel structure with α-$[Hf_2N_2]$ as building units.

EXPERIMENTAL SECTION

α-HfNBr was prepared by the reaction of Hf metal with NH_4Br, followed by purification by chemical transport.[21−23] The lattice parameters and the atomic coordinates of the obtained α-HfNBr were determined by the Rietveld analysis and are shown in Table 1. They

Table 1. Lattice Parameters and Atomic Coordinates of α- and β-Hf_2N_2S and the Pristine α-HfNBr

	α-HfNBr	α-Hf_2N_2S	β-HfNBr[a]	β-Hf_2N_2S
		Lattice Parameters		
space group	*Pmmn*	*Immm*	$R\bar{3}m$	$P\bar{3}m1$
a (Å)	4.1177(2)	4.1422(1)	3.6094(4)	3.5805(1)
b (Å)	3.5612(1)	3.5058(1)	3.6094(4)	3.5805(1)
c (Å)	8.6413(2)	11.4043(3)	29.292(4)	6.4063(1)
d (Å)[b]	8.6413(2)	5.7021(2) (= *c*/2)	9.764(1) (= *c*/3)	6.4063(1)

α-HfNBr

atom	Wyckoff site	*x*	*y*	*z*	occ	*B*/Å^2
Hf	2b	1/4	3/4	0.1015(2)	1	3.5(1)
N	2a	1/4	1/4	0.947(9)	1	1.5(8)
Br	2a	1/4	1/4	0.3390(3)	1	3.6(1)

R_{wp}, R_{exp}, R_P, R_{Bragg} (%): 4.13, 1.98, 2.87, 3.1

α-Hf_2N_2S

atom	Wyckoff site	*x*	*y*	*z*	occ	*B*/Å^2
Hf	4j	1/2	0	0.6736(1)	1	0.5(1)
N	4i	0	0	0.294(1)	1	1.0(4)
S	2a	0	0	0	1	0.3(1)

R_{wp}, R_{exp}, R_P, R_{Bragg} (%): 3.04, 1.41, 2.30, 2.3

β-Hf_2N_2S

atom	Wyckoff site	*x*	*y*	*z*	occ	*B*/Å^2
Hf	2d	1/3	2/3	0.2966(1)	1	0.40(2)
N	2d	1/3	2/3	0.681(2)	1	4.2(8)
S	1a	0	0	0	1	0.8(1)

R_{wp}, R_{exp}, R_P, R_{Bragg} (%): 3.13, 1.60, 2.19, 2.1

[a]Lattice parameters reported in ref 27. [b]*d*: basal spacing.

are in good agreement with the parameters reported by Oró-Solé et al.[21] α-HfNBr was mixed with Na_2S in a molar ratio of 2:1 and vacuum-sealed in a quartz glass tube, which was heated in various conditions in a temperature range of 700−900 °C. The reaction products were washed with water to remove soluble components such as NaBr and Na_2S, followed by drying in air. Chemical compositions were determined using an electron probe microanalyzer (EPMA) with a wavelength-dispersive X-ray spectrometer (JEOL, JCMA-733) on the samples polished in epoxy resin to avoid topographic effect. The powder X-ray diffraction (XRD) pattern was measured using an imaging plate (IP) Guinier camera (Huber G670) with monochromated Mo Kα1 (λ = 0.70926 Å) radiation and a rotating goniometer. The sample was sealed in a thin Pyrex glass capillary with a diameter of about 0.3 mm. The powder pattern was analyzed by the Rietveld program TOPAS-Academic;[24] absorption correction of the capillary sample for a parallel primary beam and preferred orientation correction based on spherical harmonics according to Järvinen were applied.[25] Optical absorption spectra were measured on the powder sample using an integral reflection sphere (Perkin-Elmer Lambda 900). Electronic band structure was calculated using the program CASTEP with the GGA-PBE (generalized gradient approximation, Perdew−Burke−Ernzehof) functional and ultrasoft potentials; a 6 × 6 × 4 Monkhorst Pack mesh was used for k-point sampling with the Brillouin zone of the orthorhombic unit cell.

RESULTS AND DISCUSSION

The Rietveld analysis was carried out on the powder sample derived from α-HfNBr by the reaction with Na_2S at 750 °C for 2 days. The analysis results are shown in Figure 2, and the

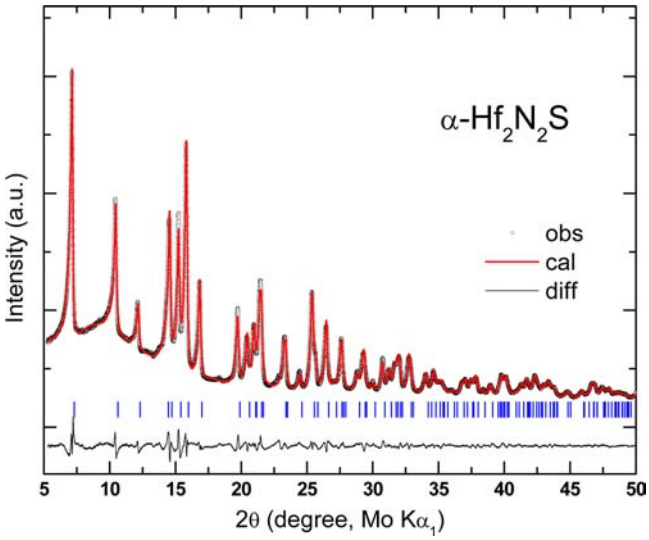

Figure 2. Rietveld analysis of the X-ray diffraction pattern of the α-type Hf_2N_2S. Open circles and solid line represent the observed data and the calculated diffraction pattern, respectively. The tic marks are calculated 2θ angles for the Bragg peaks of α-type Hf_2N_2S.

crystallographic parameters refined are compared with those of α-HfNBr in Table 1. Some selected bond lengths and angles in α-HfNBr and α-Hf_2N_2S are listed in Table 2. The EPMA

Table 2. Selected Bond Lengths and Angles in α-HfNBr and α-Hf_2N_2S along the Directions Parallel to the *a* ($\|a$) and *b* ($\|b$) Axes

	α-HfNBr	α-Hf_2N_2S
Selected Bonds (Å)		
Hf−N ($\|a$)	2.10(2)	2.104(3)
Hf−N ($\|b$)	2.23(5)	2.23(1)
Hf−Br/Hf−S	2.717(2)	2.645(1)
Selected Angles (deg)		
N−Hf−N ($\|a$)	157.0(6)	159.7(3)
N−Hf−N ($\|b$)	106.3(6)	103.9(3)
N−Hf−Br/N−Hf−S	85.9(5)	86.5(3)

analysis result of the composition of the powder sample is shown in Table 3. The Zr content of 1.55% is due to the contamination in Hf metal, and a content of 3.13% of oxygen is due to a partial hydrolysis of the sample during washing with water. The sample is not stable in an alkaline solution. It is assumed that the oxygen is combined with Hf metal as HfO_2; the rest of the powder sample has a composition Hf(Zr):N:S = 1:1.03:0.56 in atomic ratio, as shown in Table 3. Although the sulfur content is slightly larger than the stoichiometric composition of Hf_2N_2S, the composition is in good agreement

dx.doi.org/10.1021/ic401548a | Inorg. Chem. 2013, 52, 10571−10575

Table 3. Composition of the Powder Sample Determined by EPMA Analysis

element	wt %	at. %	atomic ratio for HfO_2	at. % for HfO_2	at. % for α-Hf_2N_2S	atomic ratio for α-Hf_2N_2S
Hf+Zr	82.70 + 1.55	36.01 + 1.33	1	7.61	29.73	1
N	5.54	30.72			30.72	1.03
S	6.90	16.73			16.73	0.56
O	3.13	15.22	2	15.22		
total	99.82	100.0				

with the crystallographic data within the limit of accuracy of EPMA analysis. Bromine was not detected by EPMA analysis. The compound crystallizes in space group *Immm* with the lattice parameters $a = 4.1422(1)$, $b = 3.5058(1)$, $c = 11.4043(3)$ Å and $Z = 2$. The structures of α-HfNBr and α-Hf_2N_2S are compared schematically in Figure 3, based on the parameters

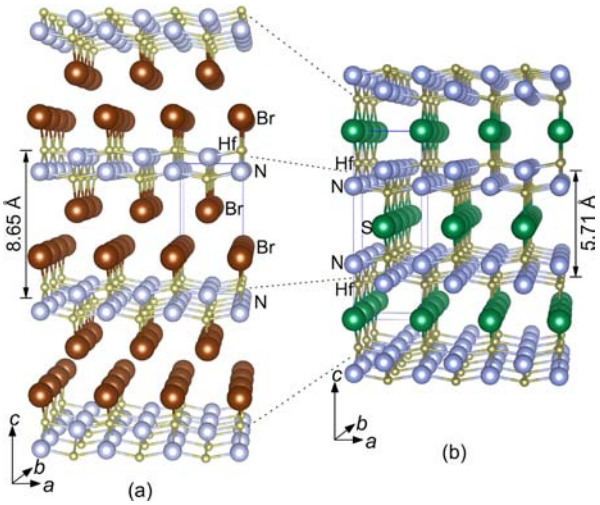

Figure 3. Crystal structures of (a) pristine α-HfNBr and (b) α-Hf_2N_2S, showing the change of the stacking of the nitride layers before and after substitution of the bromide layers with sulfide layers.

given in Table 1. Note that the structure of the α-$[Hf_2N_2]$ orthogonal network is maintained before and after the reaction, and the double Br layers are replaced with single S layers. The α-$[Hf_2N_2]$ layers are mutually shifted by $(a/2 + b/2)$ to crystallize in space group *Immm* from *Pmmn* of the pristine α-HfNBr. As the result of the shift of the layers and the cross-linking with sulfur atoms, narrow channels running along the *b* axis remain between the layers.

The heating procedure of the mixture of α-HfNBr and Na_2S was found to be essentially important to obtain α-Hf_2N_2S as a single phase. The reactant mixture should be heated rapidly to 750 °C using a preheated furnace. If the mixture was slowly heated from room temperature to 750 °C, a mixture of the α- and β-types was obtained. β-Hf_2N_2S has the La_2O_2S structure (space group $P\bar{3}m1$) with β-$[Hf_2N_2]$ double-honeycomb layers. When the reaction temperature is higher than 800 °C, the resulting compound is the β-type Hf_2N_2S. The obtained α-type Hf_2N_2S is transformed irreversibly to the β-type structure by annealing at temperatures above 850 °C for 10 h. Stoltz et al. derived two polytypes of Zr_2N_2S based on β-ZrNCl by a similar reaction with Na_2S and named them α- (space group $P\bar{3}m1$) and β-type (space group $P6_3/mmc$) with stacking of the β-$[Zr_2N_2]S$ layers in *AAAA* and *ABAB*, respectively.[18] "α-Zr_2N_2S" named by Stoltz et al. corresponds to the β-type obtained in this study. Figure 4 shows the result of the Rietveld analysis for

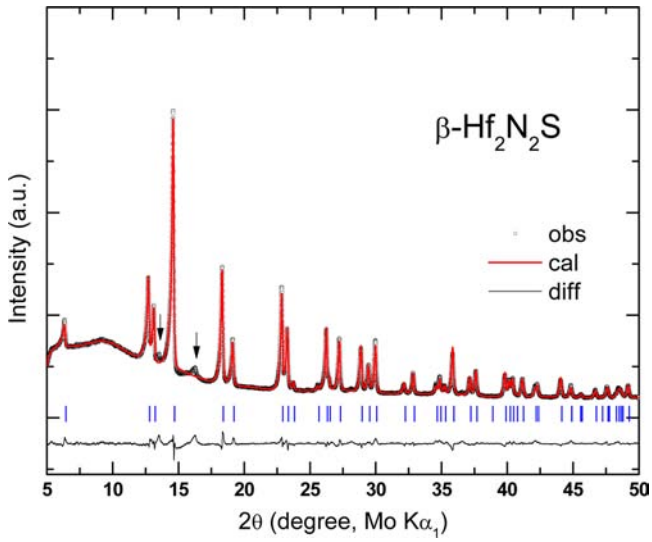

Figure 4. Rietveld analysis of the X-ray diffraction pattern of the β-type Hf_2N_2S. Open circles and solid line represent the observed data and the calculated diffraction pattern, respectively. The tic marks are calculated 2θ angles for the Bragg peaks of the β-type Hf_2N_2S. The arrows denote the reflection peaks of the other polytype of β-Hf_2N_2S with the space group $P6_3/mmc$.

β-Hf_2N_2S obtained at 800 °C. The refined crystallographic parameters are summarized in Table 1. Note that the formation of a small amount of the other polytype (space group $P6_3/mmc$) of the β-type layered structure was detected in the XRD pattern of Figure 4. Recently Lissner et al. prepared the β-type Zr_2N_2Se isomorphous with β-Hf_2N_2S by a direct reaction of a mixture of ZrN and Se in a sealed glass tube at 900 °C.[26]

It is well known that α-MNCl (M = Zr, Hf) and α-ZrNBr are thermally transformed to the corresponding β-types under ambient pressure. α-HfNBr and α-MNI (M = Zr, Hf) can be transformed to the β-type only under high pressure.[27,28] In the α-type structure, the metal atoms are six-coordinated by four nitrogen and two halogen atoms, whereas in the β-type structure, the metal atoms are seven-coordinated by four nitrogen and three halogen atoms. The β-type can be characterized as a high-pressure phase. We have selected α-HfNBr as an MNX compound thermally stable in the structure against heating in the reaction with Na_2S. The thermal transformation of α-Hf_2N_2S to the β-type is analogous to the thermal transformation of α-HfNCl and -ZrNBr to the β-type analogues. A partial substitution of Br atoms with S atoms during the reaction with Na_2S appears to generate a local stress in the layers and induce a phase transition to form β-Hf_2N_2S. The detailed mechanism is not clear.

The optical absorption spectrum of α-Hf_2N_2S was measured by using an integral reflection sphere. The spectrum is shown in Figure 5. A steep band absorption edge was observed at ~420 nm, corresponding to an optical band gap of 2.9 eV. The band gap of α-HfNBr was similarly determined to be 3.1 eV (~400

dx.doi.org/10.1021/ic401548a | *Inorg. Chem.* 2013, 52, 10571−10575

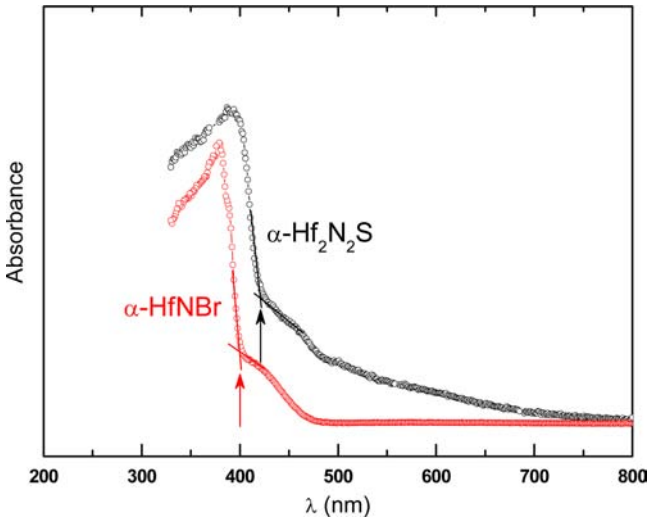

Figure 5. Optical absorption spectra of the powder samples of the α-type Hf_2N_2S compared with that of the pristine α-HfNBr.

nm) as compared in the same figure. The electronic band structures were calculated for α-Hf_2N_2S and α-HfNBr using the *ab initio* program CASTEP. The calculated band structure and the density of states (DOS) are shown in Figures 6 and 7. As

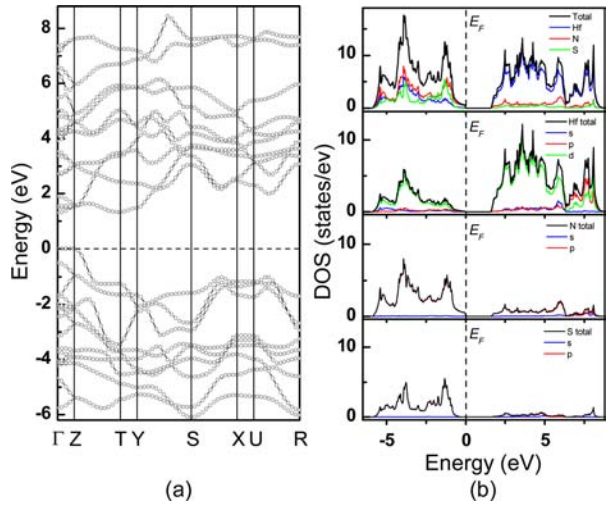

Figure 6. Band structure (a) and DOS profile (b) of α-Hf_2N_2S; total (solid line, black) and orbital-projected partial DOS for each atom.

can be seen from the figures, both compounds have direct band gaps of 1.3−1.5 eV at the Γ point, corresponding to the steep optical absorption edges observed in Figure 5. Woodward et al. calculated the band structure of the α-type MNX (M = Zr, Ti; X = Cl, Br, I) using an extended Hückel method, which also had direct gaps at the Γ point.[29] Since *ab initio* calculation usually underestimates a band gap by 1−1.5 eV, the observed values (2.9−3.1 eV) appear to be within a reasonable range. The similarity between band structures of α-HfNBr and α-Hf_2N_2S suggests that the substitution of Br with S layers hardly influences the band structures of the $[Hf_2N_2]$ units.

Figure 8 shows the arrangements of sulfur atoms in the *ab* planes of α- and β-Hf_2N_2S. The sulfur atoms are designated as spheres with a van der Waals radius of 1.80 Å. Since the *a* lattice parameter of β-Hf_2N_2S is 3.58 Å, the sulfide ions are closely packed in the interlayer space. On the other hand, the

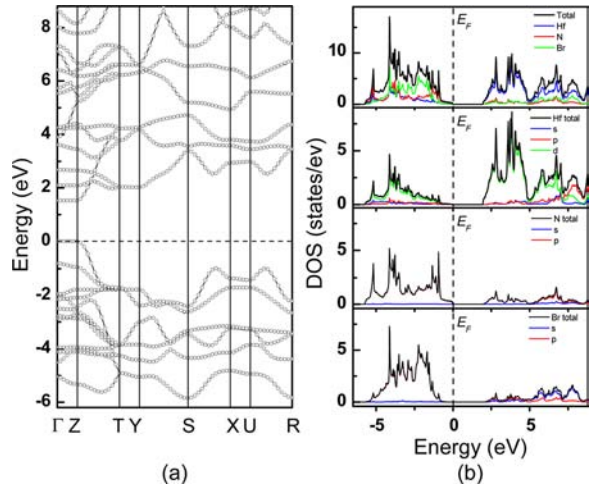

Figure 7. Band structure (a) and DOS profile (b) of α-HfNBr; total (solid line, black) and orbital-projected partial DOS for each atom.

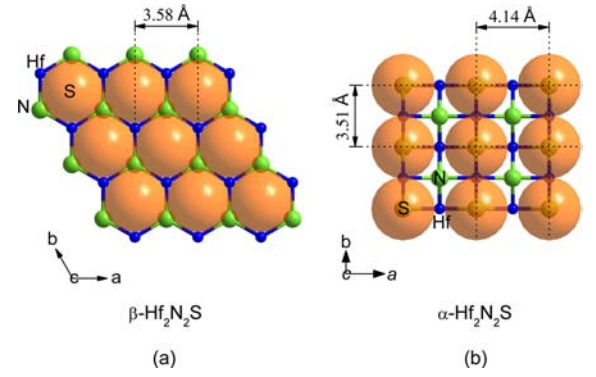

Figure 8. Schematic structural illustrations showing the arrangements of sulfur atoms with a van der Waals radius of 1.84 Å within the *ab* planes of (a) β- and (b) α-Hf_2N_2S. Sulfur atoms in α-Hf_2N_2S are more loosely packed, and narrow tunnels are formed along the *b* axis.

lattice parameters of α-Hf_2N_2S are a = 4.1422(1) and b = 3.5058(1) Å, and thus narrow tunnels running along the *b* direction remain between the layers. The areas assigned to one sulfur atom in the *ab* planes are calculated to be 14.52 and 11.18 $Å^2$ for α- and β-Hf_2N_2S, respectively. It seems possible to intercalate small cations such as Li into the tunnels along the *b* axis. We have tried to intercalate lithium into the tunnels using lithiation reagents such as *n*- and *tert*-butyllithium, and a Li-naphthalene solution in THF, which have been used for the intercalation reaction with β-ZrNCl and HfNCl.[14,30−32] However, the intercalation has not yet succeeded. It is under investigation to develop new superconductors.

CONCLUSIONS

The α-type hafnium nitride layers $[Hf_2N_2]$ of α-HfNBr are cross-linked with sulfur atoms, keeping the α-type layered structure. Narrow tunnels are formed between the layers. In the synthesis, a thermal procedure is important to obtain the compound as a single phase. The β-type variant with β-$[Hf_2N_2]$ layers is formed when the reaction temperature is too high. The preparation of intercalation compounds using tunnels is an interesting subject for future study to develop new superconductors.

dx.doi.org/10.1021/ic401548a | *Inorg. Chem.* 2013, 52, 10571−10575

AUTHOR INFORMATION

Corresponding Author

*E-mail: syamana@hiroshima-u.ac.jp. Phone: +81 (0)824-24-7740. Fax: +81 (0)824-24-7740.

Notes

The authors declare no competing financial interest.

ACKNOWLEDGMENTS

This work has been supported by the Japan Society for the Promotion of Science (JSPS) through its "Funding Program for World-Leading Innovative R&D on Science and Technology (FIRST) Program".

REFERENCES

(1) Juza, R.; Heners, J. *Z. Anorg. Allg. Chem.* **1964**, *332*, 159−172.
(2) Yamanaka, S. *Annu. Rev. Mater. Sci.* **2000**, *30*, 53.
(3) Schurz, C. M.; Shlyk, L.; Schleid, T.; Niewa, R. *Z. Kristallogr.* **2011**, *226*, 395−416.
(4) Ohashi, M.; Yamanaka, S.; Hattori, S. *J. Ceram. Soc. Jpn., Int. Ed.* **1989**, *97*, 1175.
(5) Felser, C.; Seshadri, R. *J. Mater. Chem.* **1999**, *9*, 459−464.
(6) Yamanaka, S.; Hotehama, K.; Kawaji, H. *Nature* **1998**, *392*, 580.
(7) Fogg, M. A.; Green, M. V.; O'Hare, D. *J. Mater. Chem.* **1999**, *9*, 1547−1551.
(8) Takano, T.; Kishiume, T.; Taguchi, Y.; Iwasa, Y. *Phys. Rev. Lett.* **2008**, *100*, 247005.
(9) Zheng, Z.; Yamanaka, S. *Chem. Mater.* **2011**, *23*, 1558.
(10) Ye, G.; Ying, J.; Yan, Y.; Luo, X.; Cheng, P.; Xiang, Z.; Wang, A.; Chen, X. *Phys. Rev. B* **2012**, *86*, 134501.
(11) Zhang, S.; Tanaka, M.; Onimaru, T.; Takabatake, T.; Isikawa, Y.; Yamanaka, S. *Supercond. Sci. Technol.* **2013**, *26*, 045017.
(12) Yamanaka, S. *J. Mater. Chem.* **2010**, *20*, 2922−2933.
(13) Yamanaka, S.; Umemoto, K.; Zheng, Z.; Suzuki, Y.; Matsui, H.; Toyota, N.; Inumaru, K. *J. Mater. Chem.* **2012**, *22*, 10752−10762.
(14) Zhang, S.; Tanaka, M.; Yamanaka, S. *Phys. Rev. B* **2012**, *86*, 024516.
(15) Kasahara, Y.; Kishiume, T.; Takano, T.; Kobayashi, K.; Matsuoka, E.; Onodera, H.; Kuroki, K.; Taguchi, Y.; Iwasa, Y. *Phys. Rev. Lett.* **2009**, *103*, 077004.
(16) Yin, Q.; Ylvisaker, E. R.; Pickett, W. E. *Phys. Rev. B* **2011**, *83*, 014509.
(17) Hotehama, K.; Koiwasaki, T.; Umemoto, K.; Yamanaka, S.; Tou, H. *J. Phys. Soc. Jpn.* **2010**, *79*, 014707.
(18) Stoltz, C.; Ramesha, K.; Sirchio, S. A.; Gönen, Z. S.; Eichhorn, B. W.; Salamanca-Riba, L.; Gopalakrishnan, J. *J. Am. Chem. Soc.* **2003**, *125*, 4285−4292.
(19) Franzen, H. F.; Graham, J. *J. Inorg. Nucl. Chem.* **1966**, *28*, 377−380.
(20) Franzen, H. F.; Graham, J. *Z. Kristallogr.* **1966**, *123*, 133−138.
(21) Oró-Solé, J.; Vlassov, M.; Beltrán-Porter, D.; Caldés, M. T.; Primo, V.; Fuertes, A. *Solid State Sci.* **2002**, *4*, 475−480.
(22) Yamanaka, S.; Okumura, H.; Zhu, L. *J. Phys. Chem. Solids* **2004**, *65*, 565−569.
(23) Ohashi, M.; Yamanaka, S.; Sumihara, M.; Hattori, M. *J. Solid State Chem.* **1988**, *75*, 99−104.
(24) Coelho, A. *TOPAS-Academic, V. 4.1: General Profile and Structure Analysis Software for Powder Diffraction Data*; Brisbane, Australia, 2007.
(25) Järvinen, M. *J. Appl. Crystallogr.* **1993**, *26*, 525−531.
(26) Lissner, F.; Hack, B.; Lerch, M.; Schleid, T. *Z. Anorg. Allg. Chem.* **2012**, *638*, 1407−1410.
(27) Yamanaka, S.; Itoh, K.; Fukuoka, H.; Yasukawa, M. *Inorg. Chem.* **2000**, *39*, 806−809.
(28) Chen, X.; Fukuoka, H.; Yamanaka, S. *J. Solid State Chem.* **2002**, *163*, 77−83.
(29) Woodward, P.; Vogt, T. *J. Solid State Chem.* **1998**, *138*, 207−219.
(30) Yamanaka, S.; Kawaji, H.; Hotehama, K.; Ohashi, M. *Adv. Mater.* **1996**, *8*, 771−774.
(31) Fuertes, A.; Vlassov, M.; Beltrán-Porter, D.; Alemany, P.; Canadell, E.; Casañ-Pastor, N.; Palacín, M. R. *Chem. Mater.* **1999**, *11*, 203−206.
(32) Ito, T.; Fudamoto, Y.; Fukaya, A.; Gat-Malureanu, I. M; Larkin, M. I.; Russo, P. L.; Savici, A.; Uemura, Y. J.; Groves, K.; Breslow, R.; Hotehama, K.; Yamanaka, S.; Kyriakou, P.; Rovers, M.; Luke, G. M.; Kojima, K. M. *Phys. Rev. B* **2004**, *69*, 134522.